

Thermal hysteresis in spin-crossover compounds studied within the mechanoelastic model and its potential application to nanoparticles

Laurentiu Stoleriu,¹ Pradip Chakraborty,² Andreas Hauser,² Alexandru Stancu,¹ and Cristian Enachescu^{1,*}

¹*Department of Physics, Alexandru Ioan Cuza University, Iasi, Romania*

²*Département de Chimie Physique, Université de Genève, Switzerland*

(Received 11 June 2011; published 11 October 2011)

The recently developed mechanoelastic model is applied to characterize the thermal transition in spin-crossover complexes, with special attention given to the case of spin-crossover nanoparticles. In a two-dimensional system, hexagonal-shaped samples with open boundary conditions are composed of individual molecules that are linked by springs and can switch between two states, namely, the high-spin (HS) and the low-spin (LS) states. The switching of an individual molecule during the spin transition is decided by way of a Monte Carlo standard procedure, using transition probabilities depending on the temperature, the energy gap between the two states, the enthalpy difference, the degeneracy ratio, and the local pressure determined by the elongation or compression of its closest springs. The influence of external parameters, such as temperature sweeping rate and pressure, or intrinsic features of the system, such as the value of its spring constant, on the width of the thermal hysteresis, its shape, and its position are discussed. The particular case of spin-crossover nanoparticles is treated by considering them embedded into a polymer environment, which essentially affects the molecules situated at the edges and faces by decreasing their transition probabilities from HS to LS. Finally, the pressure hysteresis, obtained by varying the external pressure at constant temperature is discussed.

DOI: [10.1103/PhysRevB.84.134102](https://doi.org/10.1103/PhysRevB.84.134102)

PACS number(s): 75.30.Wx, 64.60.-i, 75.60.-d

I. INTRODUCTION

The thermal spin transition in spin-crossover complexes belonging to the class of molecular magnets from the low-spin (LS) state at low temperature to the high-spin (HS) state at elevated temperatures has been the subject of many studies in recent years.¹⁻⁴ Depending on the strength of intermolecular interactions, the thermal transition can be gradual or it can be accompanied by a hysteresis, which makes corresponding compounds interesting for possible high-density information storage systems of the future.⁵

Spin transition molecules and complexes are composed of transition-metal ions having four to seven electrons in their valence d shell situated in an octahedral ligand field, which splits the d orbitals into antibonding e_g and weakly bonding t_{2g} orbitals. Due to a higher occupancy of the e_g orbitals in HS molecules, their molecular volume is larger than that of LS molecules.⁶ The difference in molecular volume between the two possible spin states induces distortions of the sample lattice during the transition. These distortions are at the origin of intermolecular interactions that are treated here as connecting springs, which can be either compressed or elongated relative to their length at equilibrium depending on the relative positions of neighbor molecules. The macroscopic state of the switchable system is usually characterized by the fraction of spin-crossover units in the HS state called HS fraction and denoted here as n_{HS} .

In the past, research efforts were dedicated to establish how the interactions between molecules influence the static and dynamic properties of spin-crossover solids. Using phenomenological interaction parameters, acting similarly for all molecules, the ensuing mean-field models were used to reproduce several of the characteristic features of spin-crossover compounds, such as the dependence of the thermal hysteresis width on intermolecular interactions,⁷⁻⁹ or the shift of the thermal transition toward higher temperatures^{10,11}

when applying external pressure. However, these simple models do not distinguish between short-range and long-range interactions, and therefore do not allow an advanced analysis of the hysteresis loops, nor are they able to explain how the effect of the individual switch of molecules spreads through the entire solid. In addition, these models cannot be applied for the study of size effects in nanoparticulate spin-crossover systems. Considering the cooperativity as the result of changes of the volume, shape, and elasticity of the lattice during transition, Spiering and co-workers introduced the concept of “image pressure” in their model of lattice expansion and elastic interactions.¹²⁻¹⁴ In a related approach, in his elastic models, Kambara discussed the effect of cooperative molecular distortions and lattice strains.¹⁵ However, due to the extensive calculations and experimental data required, these well-elaborated but sophisticated models have been less frequently used for interpreting spin transition curves. Ising-like models, taking into account simultaneously short- and long-range interactions have been equally proposed.¹⁶⁻¹⁹ They led to the conclusion that while long-range interactions act rather on the width of the hysteresis loop, the short-range effect is essentially visible through the steepness of the thermal hysteresis loop and the occurrence of steps. Another approach is based on the hypothesis that the spin transition occurs through concerted switching of domains of molecules in a given spin state,²⁰ allowing the reproduction of experimentally observed minor hysteresis loops by considering different inter- or intradomain interactions in the Preisach model²¹ or using the first-order reversal curves (FORC) technique.²²

The mechanoelastic model belongs to a recently developed family of elastic models based on the so-called ball and spring concept. They are based on the realistic idea that the difference of molecular volumes in the two states is at the origin of elastic interactions and induces a shift of the molecules in the system during the transition (and consequently a different volume of the entire system for every different value of

n_{HS}). In the present mechanoelastic model the problem of interactions is simplified with the use of a single interaction parameter, namely, the elastic spring constant, from which all other parameters considered in the above-mentioned models follow. Such a ball and spring model, using the molecular dynamics approach, has been applied for studying various processes such as the thermal and pressure hysteresis or relaxation phenomena in continuous^{23–27} and open boundary systems.^{28,29} The mechanoelastic model was first introduced for the study of HS-LS relaxation processes.³⁰ It was subsequently adapted for the study of photophysical processes including the phenomenon of a light-induced hysteresis,³¹ and for the study of the evolution of clusters during the thermal transition,³² or for clarifying the role of impurities during the transition.³³ Although different by their approach and method, both the molecular dynamics and the mechanoelastic model led to similar conclusions and, particularly, using open boundary conditions are able to reproduce the cluster formation starting from edges or corners, in accordance with experimental data.³⁴

In the present paper, we adapt the mechanoelastic model³⁰ for the study of the thermal transition in both directions using appropriate switching probabilities. We first present the model, then we analyze how the results are influenced by the temperature sweeping rate (number of Monte Carlo steps per K), and by the interaction strength. A further important aspect of this paper concerns the size dependence of the thermal hysteresis. In order to reproduce the experimental hysteresis measured for spin-crossover nanoparticles, we consider the samples as embedded in a polymer fixed matrix, which interacts with molecules situated at the edges. Finally, we analyze the influence of an external pressure on the thermal hysteresis as well as the pressure hysteresis obtained by varying the external pressure at an appropriate constant temperature.

II. THE MODEL

In the present model, the two-dimensional hexagonal samples with open boundary conditions are composed of spin-crossover units, in the following referred to as molecules, interacting by way of elastic connecting springs. Besides the fact that the hexagonal system is by far more stable than corresponding triangular or rectangular lattices, this planar hexagonal structure corresponds to the one of the recently well-documented two-dimensional polymeric $[\text{Fe}(\text{btr})_3](\text{ClO}_4)_2$ spin-crossover compound.^{35,36}

The model starts from the following idea: when a molecule switches from one state to the other, its volume varies, as we have stated in the Introduction. This variation will produce, at first, an instantaneous force in the springs connecting the switching molecule with its closest neighbors. This force will determine the shift in position of these neighbors and subsequently of all molecules in the system.

By this procedure, the effect of one single switch will propagate progressively through the whole sample. As a consequence, the intermolecular interactions, built in this manner as short-range interactions, affect not only the neighboring molecules but equally molecules situated at long-range distances. This is opposite to the case of the classical short-range Ising-like model applied to spin-crossover solids

where the interactions affect only the closest molecules.^{16–18} However, the intensity of the effect will be somewhat larger for molecules closer to the one having switched to the other state.

After every individual switching, all the molecules in the system start an oscillatory-type motion, which, in the absence of any damping, would continue forever. As we are interested in finding the new mechanical equilibrium state, we consider that every molecule has a damped oscillatory-type motion and we iteratively solve the following system of coupled differential equations for all molecules in the system:

$$\begin{aligned} m \frac{d^2 x_i}{dt^2} &= F_{xi} - \mu \frac{dx_i}{dt}, \\ m \frac{d^2 y_i}{dt^2} &= F_{yi} - \mu \frac{dy_i}{dt}, \end{aligned} \quad (1)$$

until the maximum change in position of any molecule between two consecutive steps is smaller than a given threshold value. The following notations have been used: x_i, y_i are the Cartesian coordinates of molecule i , μ is the damping constant, and F_{xi}, F_{yi} are the x and y components of the instantaneous force \vec{F}_i acting on particle i given by the sum of the forces from the neighboring springs:

$$\begin{aligned} F_{i,x} &= \sum_{\substack{\text{neighbors} \\ \text{springs}}} k \delta r_{ij,x}, \\ F_{i,y} &= \sum_{\substack{\text{neighbors} \\ \text{springs}}} k \delta r_{ij,y}, \end{aligned} \quad (2)$$

where k is the spring constant, and $\delta \vec{r}_{ij}$ is the deviation of the neighbor spring j from its unstressed value.

At mechanical equilibrium the following condition must always be respected:

$$\sum_{\substack{\text{neighbors} \\ \text{springs}}} k \delta \vec{r}_{ij} = 0. \quad (3)$$

As a result of this procedure, the shape of the system is perfectly hexagonal only for the limiting situations when $n_{\text{HS}} = 0$ (all the molecules in the LS state) or $n_{\text{HS}} = 1$ (all the molecules in the HS state), and elsewhere it is distorted (see Fig. 1).

Having clarified the consequences of the switching of one molecule on the lattice, we need to figure out the switching probabilities. As the HS state has a larger volume, the LS state is expected to be favored for a molecule connected with its neighbors by way of compressed springs, and vice versa, the HS state is expected to be favored for the case of a molecule surrounded by elongated springs. Therefore, the concept of local pressure as average force per unit area acting on a given molecule can be defined as

$$p_i = \sum_{\substack{\text{neighbors} \\ \text{springs}}} k \delta r_{ij}. \quad (4)$$

In Eq. (4), $\sum \delta r_{ij}$ is the algebraic sum at mechanical equilibrium of elongations and compressions of neighboring springs; that is, δr_{ij} is taken positive for compressed springs and negative for elongated ones.

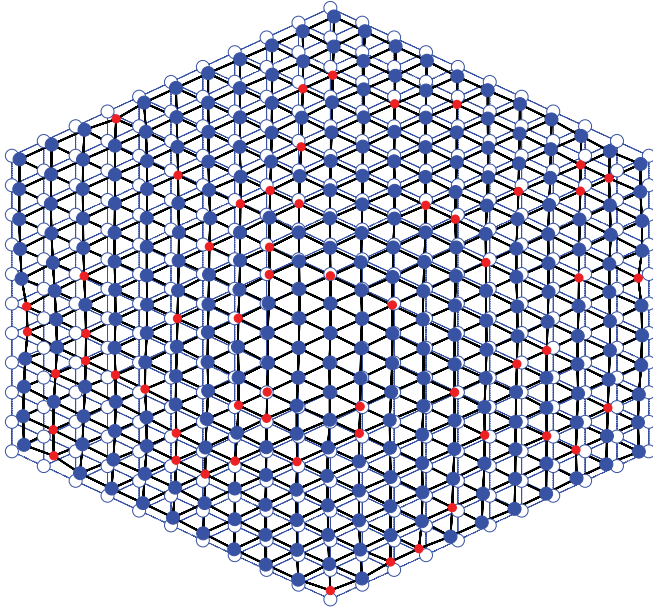


FIG. 1. (Color online) The hexagonal network of particles connected with springs (snapshot taken during the transition): big blue circles, HS molecules; small red circles, LS molecules; and open circles, HS molecules in the initial state at $n_{\text{HS}} = 1$.

The local pressure will only be the same for all molecules in the system for perfectly hexagonal-shaped systems; otherwise, the local pressures will be different for every molecule in the system. This difference in local pressure favors the formation of clusters and can lead to an avalanche phenomenon, as we have shown previously.^{30,32}

The Monte Carlo (MC) procedure employed in the model requires expressions for the transition probabilities between the two states. The individual HS \rightarrow LS and LS \rightarrow HS transition probabilities depend on the temperature, on the intrinsic features of the spin-crossover molecules, and on the interactions between molecules, represented here by way of the local pressure, according to

$$P_{\text{HS}\rightarrow\text{LS}}^i = \frac{1}{\tau} \exp\left(-\frac{E_A - \kappa p_i}{k_B T}\right), \quad (5a)$$

$$P_{\text{LS}\rightarrow\text{HS}}^i = \frac{1}{\tau} \exp\left(-\frac{D - k_B T \ln g}{k_B T}\right) \exp\left(-\frac{E_A + \kappa p_i}{k_B T}\right), \quad (5b)$$

where D is the enthalpy variation and $k_B \ln g$ is the entropy variation given by the ratio of the density of states g , E_A is the effective activation energy, T is the temperature, p_i is the local pressure acting on the i th molecule, τ is a scaling factor, chosen so that the above probabilities are well below unity at any temperature, and κ is a constant that establishes to which extent the local pressure influences the relaxation. These probabilities are similar to the probabilities used in Ref. 32 for the study of the evolution of clusters during the thermal spin transition and were determined in analogy to probabilities previously used to treat the thermal hysteresis in Ising-like models.¹³

The switch of individual molecules is checked with a standard Monte Carlo procedure. For every molecule, the

corresponding switching probability given by Eq. (5a) if the molecule is in the HS state or by Eq. (5b) if the molecule is in the LS state, is calculated, then a random number between 0 and 1 is generated. Only if this number is lower than the calculated probability, is the molecule allowed to change its state. A Monte Carlo step is completed when all the molecules in the system have been interrogated once. After every Monte Carlo step, the new mechanical equilibrium positions of all molecules are calculated.

In the simulations presented below, a 10% variation between the radius of molecules in the HS and the LS state has been assumed. However, the effect of this variation is strongly correlated with the value of the spring constant and, in turn, with the value of κ : the same results can be obtained, for example, by decreasing the radius variation with a certain factor and increasing the elastic constant or the constant κ by the same factor. The term $2\kappa p_i$ can be interpreted as an additional free-energy difference between the LS and HS states similar to the $p\Delta V_{\text{HL}}$ term in the mean-field approach for spin-crossover systems under external pressure.¹¹

Furthermore, as the local pressure term in the probabilities of Eq. (5), κp_i , can be written as $\kappa k \sum_{\text{springs}}^{\text{neighbors}} \delta r_{ij}$ using Eq. (4), the probability values are given by the product of k and κ . However, the value of k is also important for the computational time needed for the system to reach its mechanical equilibrium, after solving the system of equations (1). Therefore, for practical purposes we maintain the two parameters for the computations.

III. RESULTS AND DISCUSSIONS

A. The thermal spin transition and bistability

Figure 2 reproduces the thermal hysteresis loops for a system containing 10 981 molecules; that is, 61 molecules along each of the six edges of a hexagonal sample, for various temperature sweep rates achieved by varying the number of Monte Carlo steps per unit temperature. In the simulations we have used material parameters $D = 1100$ K, $g = 1096$, and $E_a = 400$ K, which do not correspond to a specific spin-crossover system but are in line with the values found for several spin-crossover complexes^{7,21,37} or used in Ising-like models,¹⁷ giving a thermal transition centered around 155 K. The effect of the temperature sweep rate is important not only in the simulations but also in experiments. Generally, any hysteresis is kinetic, but in many cases the lifetime of metastable states is high enough for the hysteresis to be regarded as quasistatic. For a large number of spin-crossover compounds, the intrinsic kinetics of the thermal spin-crossover phase transition are indeed quite rapid as long as the transition temperature is well above 100 K, and with only a few exceptions,³⁵ it is not possible to disentangle them from the inherent heat transfer effects under standard experimental conditions. Consequently, at least for bulk materials in the majority of cases, the experimental thermal hysteresis does not depend much on the temperature sweep rate. However, in analogy to the superparamagnetic behavior of nanometric or nanostructured magnetic systems,³⁸ this could no longer be the case for spin-crossover nanocrystals.

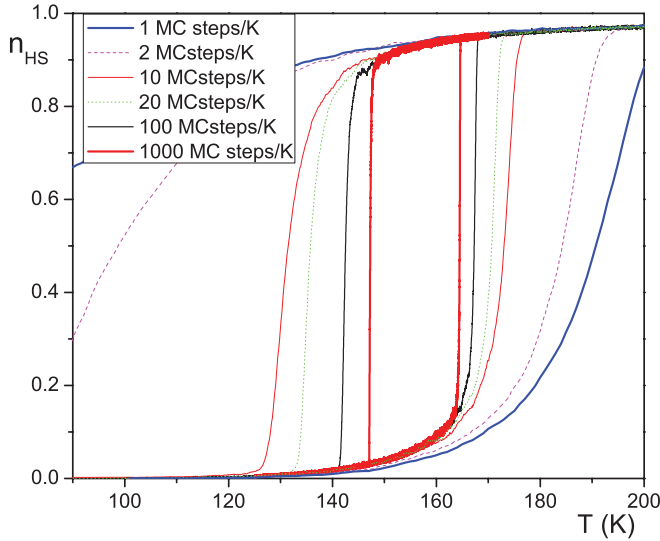


FIG. 2. (Color online) Thermal hysteresis: dependence on temperature sweep rate for a system with 10 981 molecules. The other parameters are $D = 1100$ K, $g = 1096$, $E_a = 400$ K, $\kappa = 2000$ K/N, $k = 0.7$ N/m, $k_B = 1$, and $\mu = 1$ N s/m.

From a theoretical point of view and due to the finite computing time available for finding the exact thermodynamic HS fraction at a given temperature, data obtained by Monte Carlo simulations can be affected by kinetic effects. On the one hand, this feature could be useful for studying systems composed of nanoparticles as stated above. On the other hand, it can result in an apparent hysteresis even for systems with a gradual transition and no quasistatic hysteresis.

Therefore we first establish the temperature sweep rate for which the width of the hysteresis seems to stabilize; that is, the sweep rate for which the upper and lower temperatures of the hysteresis loops approach constant values. These constant values actually correspond to spinodal points between which the metastable lifetimes diverge exponentially with a power of the system size, as discussed for elastic³⁹ or Husimi-Temperley long-range interactions.⁴⁰

As demonstrated by Fig. 2, the number of MC steps per unit temperature dramatically influences the shape and width of the thermal hysteresis. A fast temperature sweep rate results in a kinetic effect in the form of an extra broadening of the thermal hysteresis, visible particularly for the descending branch. We also notice that, for fast sweep rates, a small variation of the sweep rate results in large changes of transition temperatures and of the hysteresis width. This dependence is attenuated for comparatively lower temperature sweep rates. Consequently, in order to approach the true thermally equilibrated state of the system at a given temperature, small values of the temperature sweep rate have to be chosen.

Further insight can be gained by representing the hysteresis width on a logarithmic scale as a function of the number of MC steps per unit temperature, showing how the apparent hysteresis width decreases with an increasing number of MC steps per unit temperature (Fig. 3). The width of the hysteresis, defined as the temperature interval between upper and lower spinodal points, can be obtained by an asymptotic fit of the hysteresis width vs number of Monte Carlo steps, using for

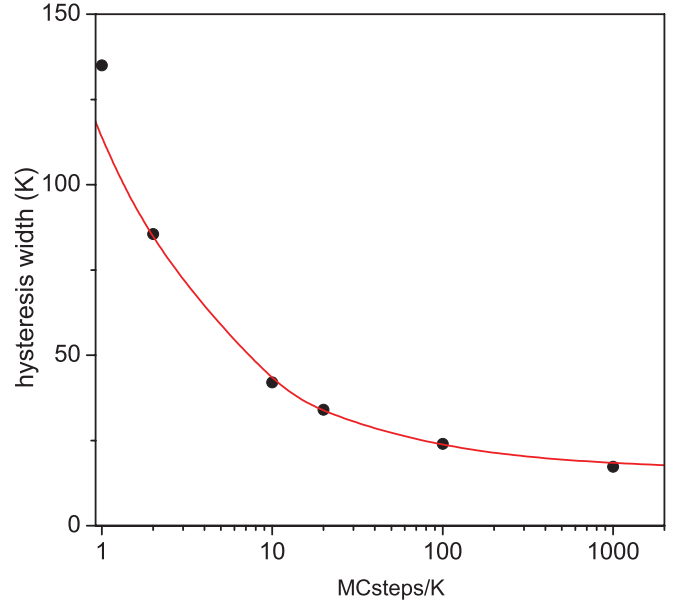


FIG. 3. (Color online) Hysteresis width dependence as a function of the temperature sweep rate on a logarithmic scale: Monte Carlo simulation (full circles), fit with a power function of type $y = A_1 x^{-p_1} + y_0$ with parameters $A_1 = 97.84$ K, $p = 0.58$, and $y_0 = 15.69$ K (full line).

example, a power function. Certainly, this function depends on a large number of parameters (system size, spring constant, etc.), but it is necessary in order to establish whether the switching temperatures are close enough to the spinodal points. From Figs. 2 and 3 it follows that for more than 100 MC steps/K, kinetic effects, resulting in an increase of the apparent hysteresis width, can be neglected. In order to maintain a reasonable computing time for the simulations we present in this paper we have chosen a sweep rate of 100 MC steps/K.

Another method to verify if the hysteresis for the lowest temperature sweep rate presented in Fig. 2 is quasistatic or not only apparent due to a still too high sweep rate, is to check for bistability around the transition temperature. This can be done by simulating relaxation curves starting from different initial HS fractions; that is, from all molecules in the HS state, all molecules in the LS state, or from arbitrary values in between. As expected, at temperatures below 148 K, that is, below the HS→LS transition for the slowest temperature sweep rate, all relaxation curves converge to a metastable state with a HS fraction close to zero [Fig. 4(a)], while at higher temperatures, that is, above the corresponding LS→HS transition at 163 K, they directly go to a value of the HS fraction close to one [Fig. 4(c)]. The switching time is longer for temperatures closer to the spinodal points. At an intermediate temperature within the hysteresis, that is, in the region of bistability, the system evolves toward one of the two states depending on the starting conditions [Fig. 4(b)]. The somewhat peculiar shape of the curves with an initial fast part followed by a plateau before the fast, sigmoidal relaxation to the final state of the system is due to the elastic interactions. In the first part the relaxation is completely random, and during the first few Monte Carlo steps at the beginning of relaxation curves small clusters of like-spin domains at the corners of the hexagon nucleate.³²

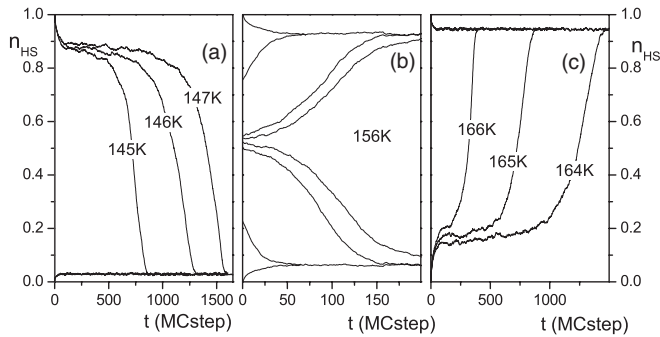


FIG. 4. Relaxation curves starting from different HS fractions inside and outside the hysteresis loop: (a) for temperatures below the quasistatic hysteresis the relaxation curves converge to HS fractions close to zero; (b) bistability inside the quasistatic thermal hysteresis loops: depending on the high spin fraction at the starting point, one of the two steady states is obtained; and (c) for temperatures higher than the quasistatic hysteresis loop the relaxation curves converge to a HS fraction close to unity.

In the plateau important fluctuations of the HS fraction may appear, until the clusters have evolved sufficiently to result in self-accelerating growth. It may be noted that experimental relaxation curves of this shape have also been reported.⁴¹

B. Dependence on the strength of the interaction

It is known that in the absence of any kind of interactions, the thermal transition is smooth and gradual and no hysteresis can be detected. As soon as the strength of intermolecular interactions is large enough, a hysteresis appears, with its shape and width depending on these interactions. In order to check the effects of the intermolecular interactions in the present model, it is necessary to study the effect of a variation of the spring constant.

As expected, we notice that the width and shape of thermal hysteresis change with the spring constant, becoming larger and more abrupt for increasing spring constants (Fig. 5). For very low elastic spring constants, the hysteresis almost vanishes. This feature is similar to the experimental situations—compounds with stronger interacting between the complexes via hydrogen bonding or $\pi\pi$ interactions present wider hysteresis—and also corresponds to numerical experiments using Ising models with stronger short-range interactions as well as the classic mean-field model. As has been previously shown using different models, bigger short-range interactions result in a squarer thermal hysteresis loop. It has also been shown that whereas strong interactions expressed by strong spring constants result in the formation of clusters both in HS \rightarrow LS relaxation curves,³⁰ as well as for the thermal hysteresis,³² lower elastic constants just below the critical value result in almost random switches inside the sample and therefore essentially reproduce the predictions of the mean-field approach.

C. Sample size dependence

As spin-crossover nanoparticles have become a hot topic in the spin-crossover community over the past few years,^{42–45} the theoretical study of the behavior of these systems is

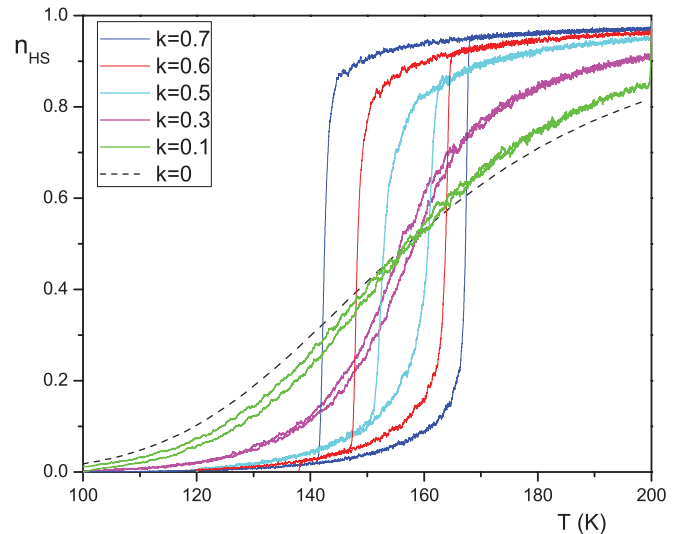


FIG. 5. (Color online) Thermal transition for various spring constant interactions. If the spring constant is higher than a threshold value, then the transition is accompanied by a hysteresis. All the parameters are those from Fig. 2, except the number of Monte Carlo steps considered at every temperature unit, which is 100 steps/K.

becoming increasingly important. The open boundary conditions considered in our model make it very appropriate for the study of nanoparticle systems, as edge effects play an important role during the thermal transition as well as for relaxation processes.

Experimental data show that, generally, nanoparticles have a different behavior compared to that of the bulk samples.⁴⁶ The reduction in size results in a smoother transition and a shift of the transition temperature toward lower temperatures. At the same time, hysteresis loops become narrower and

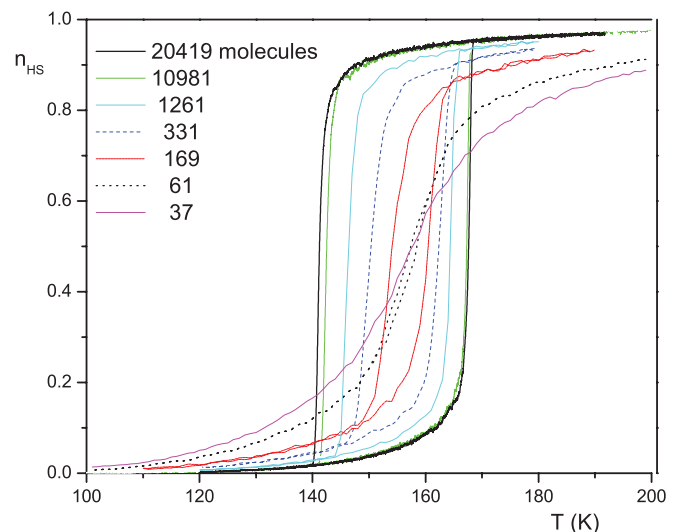


FIG. 6. (Color online) Size dependence of the thermal hysteresis for systems composed from 37 to 20419 molecules. The plotted curves corresponding to systems with less than 10 000 molecules have been obtained as the average of several calculated curves (from 10 for the system with 1261 molecules to 1000 for the system with 37 molecules). Number of Monte Carlo steps = 100 steps/K. The other parameters are those from Fig. 2.

eventually the hysteresis is replaced by a reversible curve or the transition can become incomplete if the particle size is small enough. A tentative explanation of this behavior has been given in Ref. 46 and implies that the shift of the transition toward lower temperatures is produced by the cutoff of the cooperativity because long-range interactions are limited by the open boundary conditions.

In order to study the size effects within the framework of the present model, we have performed simulations of the thermal hysteresis on samples with sizes from 37 (four molecules along each edge) up to 20 419 molecules (83 molecules along each edge). We show that, if the system size decreases, the thermal hysteresis width becomes smaller. We find that there is a critical dimension of the system, for which the hysteresis vanishes. For the present system, the critical dimension, which can be considered as the superparamagnetic limit for this system, is between 37 and 61 (four to five molecules along each edge), but, of course, this value depends on the spring constant. This observation confirms the prediction made several years ago by Oliver Kahn⁴⁷ and confirmed experimentally very recently,⁴⁸ that there is a minimum size for hysteretic behavior in spin-crossover phenomena and that this limit is expected to be around a few nanometers. In addition, compatible results have been obtained in a three-dimensional (3D) Ising-like model.⁴⁹

However, the data presented in Fig. 6 reproduce only partially experimental data: the decreasing hysteresis width with decreasing particle size is successfully reproduced, but the generally observed decrease of the transition temperature with decreasing size is not adequately simulated.

In order to account for all experimental features, and especially the decrease of the thermal transition temperature for spin-crossover nanoparticles compared to the bulk value, we consider weak interactions between spin-crossover molecules situated at the edge of the system and the surrounding medium. The motivation for this is presented in the following. In a real situation, nanoparticles are prepared either by the inverse micelle method⁴² or polymer protected synthesis⁴⁵ in order to obtain different particle sizes. The polymer itself forms a flexible matrix around the nanoparticles, thus preventing the

nanoparticles from agglomerating through the highly favorable surface free energy. On the other hand, with decreasing nanoparticle size, more and more molecules are present on the surface compared to the core (high surface-to-volume ratio). The surface molecules interact with the polymer matrix via van der Waals interactions and, depending upon the matrix, hydrogen bonding. According to the mechanoelastic model, the thermal spin transition occurs from the surface, preferentially from the corners,^{30,32} and HS to LS transformation effectively reduces the volume of the individual molecule as well as of the whole nanoparticle. As a result, the cavity provided by the polymer matrix for the nanoparticle becomes too big. However, at low temperatures the polymer matrix is much less flexible than at room temperature. Thus, in addition to the internal interactions considered by the mechanoelastic model so far, the reduction of the overall volume of the nanoparticle results in a negative contribution to the pressure originating from pulling forces from the polymer network. The absolute value of this negative pressure increases with increasing LS fraction. As shown in Fig. 7(a), we consider small nanoparticles embedded in a polymer matrix, which creates such an increasingly negative pressure on edge molecules during the transition. For the effective modeling, it proved simpler to consider that the system is enclosed by a rigid shell of nonswitching molecules attached to the spin-crossover molecules with springs of a given force constant, that we denote here as k_{pol} . These will progressively reduce the HS→LS switching probability of the molecules closer to the edge. With this premise, the transition is more gradual while the transition temperature moves to lower temperatures [Fig. 7(b), $k_{\text{pol}} = 0.007k$, for a system with 2791 molecules]. For an even higher interaction between edge molecules and the embedding polymer $k_{\text{pol}} = 0.04k$, the transition is not complete anymore, and a residual HS fraction results. In Fig. 7(c) we present three snapshots of the polymer-embedded system taken during the descending branch for different values of n_{HS} , and for comparison, a snapshot of an open boundary system at an intermediate n_{HS} value. We notice that, even if the switching probability of edge molecules is lowered due to the presence of a polymer matrix, LS clusters still start to

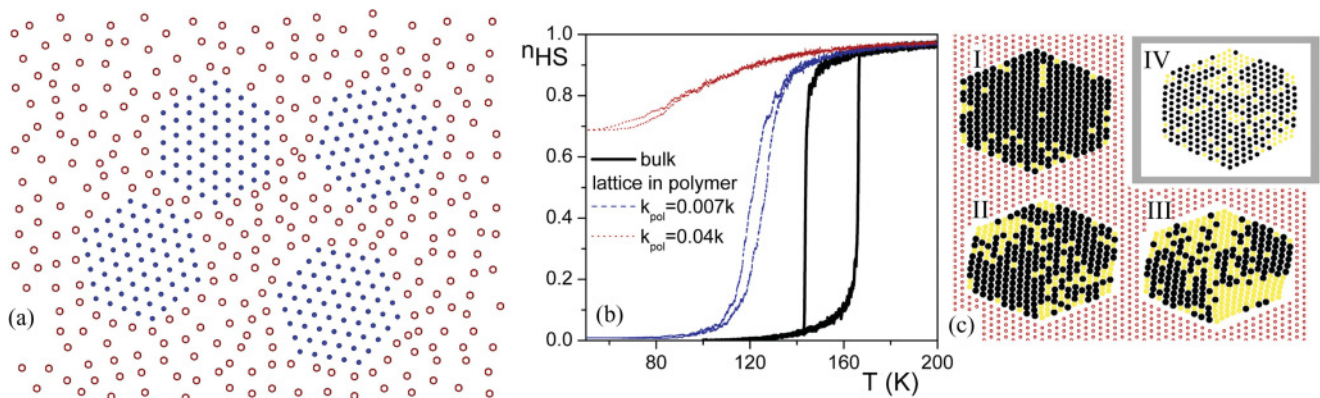


FIG. 7. (Color online) (a) Hexagonal spin-crossover nanoparticles (full circles) embedded in a polymer matrix (open circles). (b) Thermal hysteresis for bulk systems (thick full line) and nanoparticles in polymer (thin dashed and dotted lines). (c) Snapshots of spin configurations for polymer-embedded nanoparticles for $n_{\text{HS}} = 0.9$ (I), $n_{\text{HS}} = 0.7$ (II), and $n_{\text{HS}} = 0.5$ (III), and for open boundaries nanoparticles at $n_{\text{HS}} = 0.7$ (IV). Black circles, HS molecules; yellow circles, LS molecules.

form from corners, as in the case of open boundary systems. In order to obtain further insight concerning the differences between the evolution of clusters in the two types of systems, a more thorough analysis, including a comparison between the wetting angle of the nucleation droplets for various k_{pol} (Ref. 50) is necessary. This problem will be treated in a future study.

D. External pressure dependence and pressure hysteresis

While in the previous paragraphs we have analyzed the effects of a variable negative pressure on spin-crossover nanoparticles resulting from their interaction with the surrounding medium, in the following we shall discuss the case of a positive external pressure. The external pressure effect on spin-crossover complexes has been studied theoretically and experimentally in several papers^{11,51,52} (and references therein). If the external pressure increases, then the LS state is favored due to its smaller volume and the spin transition is shifted toward higher temperatures, while the width of the thermal hysteresis, if it exists, becomes smaller.

In order to take into account the external pressure in the mechanoelastic model, we have added constant pressure forces acting on particles situated at the edges of the system. The pressure forces are considered equal in their absolute values and oriented in the direction of the springs connecting the particle with its neighbors inside the lattice. This definition of the external pressure will produce an initial compression of all springs in the system (and a shift in position of all molecules in the system toward the inner regions), until the vector sum of the forces acting on all system molecules becomes zero [Eq. (4)]. In this case, the local pressure for edge molecules is written as

$$p_i = \sum_{\substack{\text{neighbors} \\ \text{springs}}} k\delta x_i + \sum_{\substack{\text{missing} \\ \text{springs}}} p, \quad (6)$$

while for all other molecules in the system the local pressure is still given by relation (3).

In Fig. 8 we present thermal hysteresis loops simulated for different external pressures. As expected according to experimental data, the hysteresis loop shifts toward higher temperatures and its width diminishes. For small external pressures applied to the system, the hysteresis width is inversely proportional to the external pressure; this is no longer the case for higher external pressures. For even higher values of the pressure, the hysteresis finally vanishes.

Besides the thermal hysteresis, another spin-crossover hysteresis of interest is the pressure hysteresis. In this case, the temperature is kept constant at a value above the thermal transition temperature where n_{HS} is close to one, while the external pressure varies in small steps. The local pressures will then vary not only as a result of the reorganization of the molecules in the system during the transition, but also as a direct effect of the external pressure. Simulated pressure hysteresis loops at constant temperature in the frame of the present model are shown in Fig. 9. The main characteristics of experimental hysteresis loops, discussed above, can also be noticed in the simulated cycles insofar as they are mirroring the hysteresis loop for the thermal hysteresis, with a HS fraction

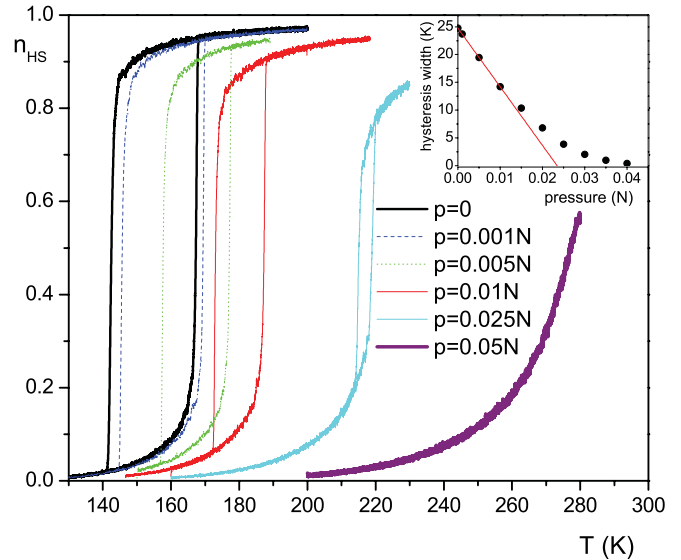


FIG. 8. (Color online) Thermal hysteresis for different external pressures. Inset: the hysteresis width as a function of external pressure. The other parameters are those given in the previous figures.

close to one at lower pressure. This is in qualitative agreement with the mean-field model, for which it was shown that any pressure hysteresis loop can be obtained from a thermal hysteresis loop by a linear variable change.⁵¹

IV. CONCLUSIONS

In this paper we have realized an extensive simulation of the main features of the thermal hysteresis in spin-crossover complexes by using the mechanoelastic model, and we have shown that experimental data can be reproduced in the framework of the present model. Special attention has been devoted to the behavior of nanosized systems, and we have shown that considering the interactions with the embedding polymer,

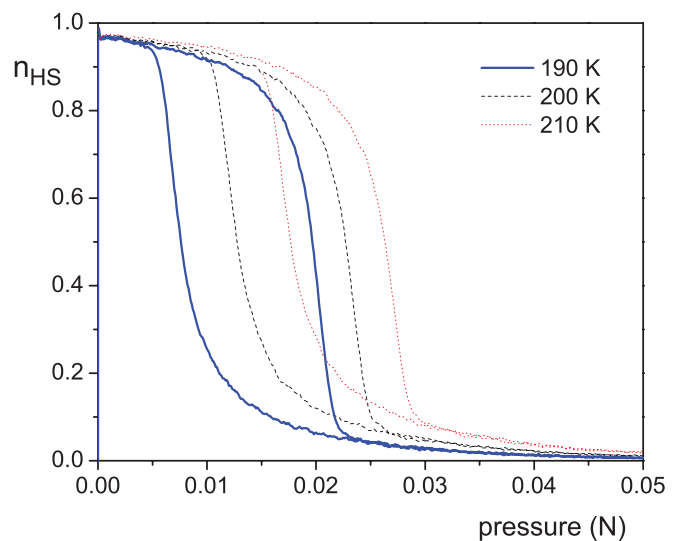


FIG. 9. (Color online) Simulated pressure hysteresis loops at constant temperatures. For lower temperature, the hysteresis is wider and shifts to lower pressures.

the particular behavior of these systems, and primarily the variation of the transition temperature with the system's size can be reproduced. The behavior of the samples under external pressure has also been discussed. In further work, we shall extend our model to 3D in order to have better insight into the behavior of spin-crossover nanoparticles.

ACKNOWLEDGMENTS

This work was supported by Romanian CNCSIS, Projects No. PNII RU-TE 185/2010 and No. PCCE 9/2010, and by the Swiss National Science Foundation (Grant No. 200020-125175).

*Corresponding author: cristian.enachescu@uaic.ro

¹P. Gütllich and H. A. Goodwin, *Spin Crossover in Transition Metal Compounds I–III* (Springer, Heidelberg, 2004).

²E. D. Loutete-Dangui, F. Varret, E. Codjovi, P. R. Dahoo, H. Tokoro, S. Ohkoshi, C. Eypert, J. F. Létard, J. M. Coanga, and K. Boukheddaden, *Phys. Rev. B* **75**, 184425 (2007).

³S. Cobo, D. Ostrovskii, S. Bonhommeau, L. Vendier, G. Molnar, L. Salmon, K. Tanaka, and A. Bousseksou, *J. Am. Chem. Soc.* **130**, 9019 (2008).

⁴S. Lakhloufi, P. Guionneau, M. H. Lemee-Cailleau, P. Rosa, and J. F. Létard, *Phys. Rev. B* **82**, 132104 (2010).

⁵J. F. Létard, P. Guionneau, and L. Goux-Capes, *Top. Curr. Chem.* **235**, 221 (2004).

⁶E. König, *Struct. Bonding* (Berlin) **76**, 51 (1991).

⁷P. Gütllich, A. Hauser, and H. Spiering, *Angew. Chem., Int. Ed.* **33**, 2024 (1994).

⁸H. Spiering, T. Kohlhaas, H. Romstedt, A. Hauser, C. Bruns-Yilmaz, J. Kusz, and P. Gütllich, *Coord. Chem. Rev.* **190-192**, 629 (1999).

⁹C. Enachescu, J. Linares, and F. Varret, *J. Phys.: Condens. Matter* **13**, 2481 (2001).

¹⁰C. P. Köhler, R. Jakobi, E. Meissner, L. Wiehl, H. Spiering, and P. Gütllich, *J. Phys. Chem. Solids* **51**, 239 (1990).

¹¹J. Jęftic and A. Hauser, *J. Phys. Chem. B* **101**, 10262 (1997).

¹²H. Spiering, E. Meissner, H. Koppen, E. W. Müller, and P. Gütllich, *Chem. Phys.* **68**, 65 (1982).

¹³H. Spiering and N. Willenbacher, *J. Phys.: Condens. Matter* **1**, 10099 (1989).

¹⁴H. Spiering, *Top. Curr. Chem.* **235**, 171 (2004).

¹⁵T. Kambara, *J. Chem. Phys.* **74**, 4557 (1981).

¹⁶A. Bousseksou, J. Nasser, J. Linares, K. Boukheddaden, and F. Varret, *J. Phys. I* **2**, 1381 (1992).

¹⁷K. Boukheddaden, I. Shteto, B. Hôo, and F. Varret, *Phys. Rev. B* **62**, 14796 (2000).

¹⁸F. Varret, S. A. Salunke, K. Boukheddaden, A. Bousseksou, E. Codjovi, C. Enachescu, and J. Linares, *C. R. Chim.* **6**, 385 (2003).

¹⁹T. Kohlhaas, H. Spiering, and P. Gütllich, *Z. Phys. B* **102**, 455 (1997).

²⁰M. Sorai, Y. Maeda, and H. Oshio, *J. Phys. Chem. Solids* **51**, 941 (1990).

²¹C. Enachescu, H. C. Machado, N. Menendez, E. Codjovi, J. Linares, F. Varret, and A. Stancu, *Physica B* **306**, 155 (2001).

²²R. Tanasa, C. Enachescu, A. Stancu, J. Linares, E. Codjovi, F. Varret, and J. Haasnoot, *Phys. Rev. B* **71**, 014431 (2005).

²³S. Miyashita, Y. Konishi, M. Nishino, H. Tokoro, and P. A. Rikvold, *Phys. Rev. B* **77**, 014105 (2008).

²⁴Y. Konishi, H. Tokoro, M. Nishino, and S. Miyashita, *Phys. Rev. Lett.* **100**, 067206 (2008).

²⁵S. Miyashita, M. Nishino, Y. Konishi, H. Tokoro, K. Boukheddaden, F. Varret, and P. A. Rikvold, *J. Phys.: Conf. Ser.* **148**, 012027 (2009).

²⁶M. Nishino, K. Boukheddaden, and S. Miyashita, *Phys. Rev. B* **79**, 012409 (2009).

²⁷M. Nishino, K. Boukheddaden, Y. Konishi, and S. Miyashita, *Phys. Rev. Lett.* **98**, 247203 (2007).

²⁸M. Nishino, K. Boukheddaden, S. Miyashita, and F. Varret, *J. Phys.: Conf. Ser.* **148**, 012034 (2009).

²⁹M. Nishino, C. Enachescu, S. Miyashita, K. Boukheddaden, and F. Varret, *Phys. Rev. B* **82**, 020409 (2010).

³⁰C. Enachescu, L. Stoleriu, A. Stancu, and A. Hauser, *Phys. Rev. Lett.* **102**, 257204 (2009).

³¹C. Enachescu, L. Stoleriu, A. Stancu, and A. Hauser, *Phys. Rev. B* **82**, 104114 (2010).

³²C. Enachescu, M. Nishino, S. Miyashita, L. Stoleriu, A. Stancu, and A. Hauser, *Europhys. Lett.* **91**, 27003 (2010).

³³C. Enachescu, L. Stoleriu, A. Stancu, and A. Hauser, *J. Appl. Phys.* **109**, 07B111 (2011).

³⁴C. Chong, F. Varret, and K. Boukheddaden, *Phys. Rev. B* **81**, 014104 (2010).

³⁵I. Krivokapic, C. Enachescu, R. Bronisz, and A. Hauser, *Chem. Phys. Lett.* **455**, 192 (2008).

³⁶I. Krivokapic, P. Chakraborty, C. Enachescu, R. Bronisz, and A. Hauser, *Angew. Chem., Int. Ed.* **49**, 8509 (2010).

³⁷A. Hauser, J. Jęftic, H. Romstedt, R. Hinek, and H. Spiering, *Coord. Chem. Rev.* **190-192**, 471 (1999).

³⁸L. Néel, *Ann. Geophys.* **5**, 99 (1949).

³⁹S. Miyashita, P. A. Rikvold, T. Mori, Y. Konishi, M. Nishino, and H. Tokoro, *Phys. Rev. B* **80**, 064414 (2009).

⁴⁰T. Mori, S. Miyashita, and P. A. Rikvold, *Phys. Rev. E* **81**, 011135 (2010).

⁴¹A. Desaix, O. Roubeau, J. Jęftic, J. G. Haasnoot, K. Boukheddaden, E. Codjovi, J. Linares, M. Nogues, and F. Varret, *Eur. Phys. J. B* **6**, 183 (1998).

⁴²I. Boldog, A. B. Gaspar, V. Martinez, P. Pardo-Ibanez, V. Ksenofontov, A. Bhattacharjee, P. Gütllich, and J. A. Real, *Angew. Chem.* **47**, 6433 (2008).

⁴³E. Coronado, J. R. Galán-Mascarós, M. Monrabal-Capilla, J. García-Martínez, and P. Pardo-Ibáñez, *Adv. Mater.* **19**, 1359 (2007).

⁴⁴T. Forestier, A. Kaiba, S. Pechev, D. Denux, P. Guionneau, C. Etrillard, N. Daro, E. Freysz, and J. F. Létard, *Chem. Eur. J.* **15**, 6122 (2009).

⁴⁵V. Martínez, I. Boldog, A. B. Gaspar, V. Ksenofontov, A. Bhattacharjee, P. Gütllich, and J. A. Real, *Chem. Mater.* **22**, 4271 (2010).

⁴⁶F. Volatron, L. Catala, E. Riviere, A. Gloter, O. Stephan, and T. Mallah, *Inorg. Chem.* **47**, 6584 (2008).

- ⁴⁷O. Kahn and C. J. Martinez, *Science* **279**, 44 (1998).
- ⁴⁸J. Larionova, L. Salmon, Y. Guari, A. Tokarev, K. Molvinger, G. Molnar, and A. Bousseksou, *Angew. Chem.* **120**, 8360 (2008).
- ⁴⁹T. Kawamoto and S. Abe, *Chem. Commun.* 3933 (2005).
- ⁵⁰H. L. Richards, M. Kolesik, P. A. Lindgard, P. A. Rikvold, and M. A. Novotny, *Phys. Rev. B* **55**, 11521 (1997).
- ⁵¹R. Tanasa, A. Stancu, E. Codjovi, J. Linares, F. Varret, and J. F. Letard, *J. Appl. Phys.* **103**, 07B905 (2008).
- ⁵²P. Gütllich, A. B. Gaspar, V. Ksenofontov, and Y. Garcia, *J. Phys.: Condens. Matter* **16**, S1087 (2004).